J|A|C|S ARTICLES

Published on Web 12/04/2009

Charge Recombination and Exciton Annihilation Reactions in Conjugated Polymer Blends

Ian A. Howard,[†,||] Justin M. Hodgkiss,[†,⊥] Xinping Zhang,[†,#] Kiril R. Kirov,[†] Hugo A. Bronstein,[‡] Charlotte K. Williams,[‡] Richard H. Friend,[†] Sebastian Westenhoff,*[,†,§] and Neil C. Greenham[†]

Cavendish Laboratory, J. J. Thomson Avenue, Cambridge CB3 0HE, United Kingdom, Department of Chemistry, Imperial College London, London SW7 2AZ, United Kingdom, and Department of Chemistry, Biochemistry & Biophysics, University of Gothenburg, Box 462, 40530 Gothenburg, Sweden

Received September 22, 2009; E-mail: westenho@chem.gu.se

Abstract: Bimolecular interactions between excitations in conjugated polymer thin films are important because they influence the efficiency of many optoelectronic devices that require high excitation densities. Using time-resolved optical spectroscopy, we measure the bimolecular interactions of charges, singlet excitons, and triplet excitons in intimately mixed polyfluorene blends with band-edge offsets optimized for photoinduced electron transfer. Bimolecular charge recombination and triplet−triplet annihilation are negligible, but exciton−charge interactions are efficient. The annihilation of singlet excitons by charges occurs on picosecond time-scales and reaches a rate equivalent to that of charge transfer. Triplet exciton annihilation by charges occurs on nanosecond time-scales. The surprising absence of nongeminate charge recombination is shown to be due to the limited mobility of charge carriers at the heterojunction. Therefore, extremely high densities of charge pairs can be maintained in the blend. The absence of triplet−triplet annihilation is a consequence of restricted triplet diffusion in the blend morphology. We suggest that the rate and nature of bimolecular interactions are determined by the stochastic excitation distribution in the polymer blend and the limited connectivity between the polymer domains. A model based on these assumptions quantitatively explains the effects. Our findings provide a comprehensive framework for understanding bimolecular recombination and annihilation processes in nanostructured materials.

1. Introduction

Bimolecular excitation dynamics influence the performance of organic optoelectronic devices that sustain high densities of excited states. In organic light-emitting diodes, including those utilizing long-lived phosphorescent dopants, exciton−exciton annihilation and exciton−charge annihilation are both significant loss mechanisms.[1−4] The pursuit of electrically pumped organic lasing requires detailed understanding of various second-order loss mechanisms, including those that affect the population of precursor charge states, the emissive singlet states, and the loss-causing triplet states.[5−7] Light-emitting organic field-effect transistors also require high charge and exciton densities within the emission zone, making bimolecular interactions likely.[8,9] Understanding whether photogenerated charge carriers recombine nongeminately (bimolecularly)[10−12] or geminately (monomolecularly)[13−18] is crucial for the improvement of organic solar cells. Finally, bimolecular excitation dynamics do not only lead

† Cavendish Laboratory.
‡ Imperial College London.
§ University of Gothenburg.
|| Current affiliation: Max Planck Institute for Polymer Research, Ackermannweg 10, D-55128 Mainz, Germany.
⊥ Current affiliation: School and Chemical and Physical Sciences and the MacDiarmid Institute for Advanced Materials and Nanotechnology, Victoria University of Wellington, P.O. Box 600, Wellington, New Zealand.
Current affiliation: College of Applied Sciences, Beijing University of Technology, Beijing 100022, People's Republic of China.

(1) Sebastian, R.; Karsten, W.; Karl, L. *Phys. Rev. B* **2007**, *75*, 125328.
(2) Adachi, C.; Baldo, M. A.; Forrest, S. R. *J. Appl. Phys.* **2000**, *87*, 8049–8055.
(3) Nakanotani, H.; Sasabe, H.; Adachi, C. *Appl. Phys. Lett.* **2005**, *86*, 213506.
(4) Staroske, W.; Pfeiffer, M.; Leo, K.; Hoffmann, M. *Phys. Rev. Lett.* **2007**, *98*, 197402.
(5) Gartner, C.; Karnutsch, C.; Lemmer, U.; Pflumm, C. *J. Appl. Phys.* **2007**, *101*, 023107.
(6) Denton, G. J.; Tessler, N.; Harrison, N. T.; Friend, R. H. *Phys. Rev. Lett.* **1997**, *78*, 733–736.
(7) Baldo, M. A.; Holmes, R. J.; Forrest, S. R. *Phys. Rev. B* **2002**, *66*, 035321.
(8) Hepp, A.; Heil, H.; Weise, W.; Ahles, M.; Schmechel, R.; von Seggern, H. *Phys. Rev. Lett.* **2003**, *91*, 157406.
(9) Zaumseil, J.; Friend, R. H.; Sirringhaus, H. *Nat. Mater.* **2006**, *5*, 69–74.
(10) Nelson, J. *Phys. Rev. B* **2003**, *67*, 155209.
(11) Montanari, I.; Nogueira, A. F.; Nelson, J.; Durrant, J. R.; Winder, C.; Loi, M. A.; Sariciftci, N. S.; Brabec, C. *Appl. Phys. Lett.* **2002**, *81*, 3001–3003.
(12) Snaith, H. J.; Arias, A. C.; Morteani, A. C.; Silva, C.; Friend, R. H. *Nano Lett.* **2002**, *2*, 1353–1357.
(13) Mihailetchi, V. D.; Koster, L. J. A.; Hummelen, J. C.; Blom, P. W. M. *Phys. Rev. Lett.* **2004**, *93*, 216601.
(14) McNeill, C. R.; Westenhoff, S.; Groves, C.; Friend, R. H.; Greenham, N. C. *J. Phys. Chem. C* **2007**, *111*, 19153–19160.
(15) Offermans, T.; Meskers, S. C. J.; Janssen, R. A. J. *J. Chem. Phys.* **2003**, *119*, 10924–10929.
(16) De, S.; Pascher, T.; Maiti, M.; Jespersen, K. G.; Kesti, T.; Zhang, F. L.; Inganas, O.; Yartsev, A.; Sundstrom, V. *J. Am. Chem. Soc.* **2007**, *129*, 8466–8472.

 10.1021/ja908046h

to losses. Triplet−triplet annihilation has been exploited to realize optical up-conversion of low-energy photons,[19−21] which could enhance the harvesting of low-energy sun light in future generations of organic photovoltaics.

Today, many organic optoelectronic devices rely on sophisticated nanoscale architectures. Recent examples include organic single-molecule transistors,[22] various systems comprising complex colloidal nanoparticle assemblies,[23] and organic solar cells,[24−26] which may have controlled mesoscale order.[27−29] In all of these devices, excitations are confined on the length scale of a few nanometers; this will alter their effective diffusivity and consequently their bimolecular interactions. It is therefore important to study and understand these bimolecular reactions within nanostructured morphologies.

In organic semiconductors, neutral excitations are generally considered to be tightly bound Frenkel excitons that may exist in the singlet or triplet manifold.[30] Neutral excitations and charged species, which are also termed radicals or polarons, are stabilized by rearrangements of the underlying molecular structure. In noncrystalline thin films, they are therefore localized on chain segments and extend only over a few molecular units.[31,32] Excitations may migrate between different chain segments,[33] and bimolecular interactions are in general limited by their diffusion constants. The characteristic time-scales for exciton transfer are picoseconds for singlet excitons, where transport is primarily through long-range Förster-type transfer,[34,35] and nanoseconds for charged and neutral triplet species, where only through-bond transfer is active.[36]

Singlet excitons, triplet excitons, and charges in conjugated materials can in principle react with each other and themselves. These reaction are termed "annihilations" because at least one of the excited species returns to the ground state. Each of these interactions has been reported in single-layer films,[6,37−48] but they have so far not been investigated in nanostructured samples. Bimolecular processes that involve singlet excitons are well-studied, because it is straightforward to probe their photoluminescence and photoinduced absorptions using femtosecond time-resolved spectroscopy. Because of their high diffusivity, singlet excitons annihilate extremely efficiently among themselves in organic semiconductors on picosecond time-scales,[6,38,39] and this is a sensitive probe of exciton mobility.[49,50] Singlet excitons may also be quenched by charges at high excitation densities.[40,41] The measurement of bimolecular processes that only involve "dark" excitations, such as triplets and charges,[51] were initially made difficult by ambiguities in the assignment of long-lived photoinduced absorption features.[52] Singlet−triplet annihilation has been reported to be significant in polyfluorene thin films,[42] but another report on a similar sample concluded exactly the opposite, that this process is insignificant.[45] Delayed fluorescence can be used to probe interactions that result in the reformation of singlet excitons, although controversy between the role of charge recombination[53] and triplet−triplet annihilation[43,44,46,47] exists in the interpretation of delayed fluorescence data. These examples highlight that further studies are necessary, especially in systems where two or more bimolecular processes may be active simultaneously. To comprehensively and quantitatively assess the relative importance of bimolecular interactions in these systems, experimental techniques should be developed, which probe specific reactions selectively.

Here, we study the bimolecular interactions of excitations in a binary polyfluorene blend,[14,54] with the band-edge offsets of the two blend components optimized for photocurrent generation

(17) Marsh, R. A.; Groves, C.; Greenham, N. C. *J. Appl. Phys.* **2007**, *101*, 083509.
(18) Westenhoff, S.; Howard, I. A.; Hodgkiss, J. M.; Kirov, K. R.; Bronstein, H. A.; Williams, C. K.; Greenham, N. C.; Friend, R. H. *J. Am. Chem. Soc.* **2008**, *130*, 13653–13658.
(19) Islangulov, R. R.; Lott, J.; Weder, C.; Castellano, F. N. *J. Am. Chem. Soc.* **2007**, *129*, 12652–12653.
(20) Keivanidis, P. E.; Baluschev, S.; Miteva, T.; Nelles, G.; Scherf, U.; Yasuda, A.; Wegner, G. *Adv. Mater.* **2003**, *15*, 2095–2098.
(21) Baluschev, S.; Yakutkin, V.; Miteva, T.; Wegner, G.; Roberts, T.; Nelles, G.; Yasuda, A.; Chernov, S.; Aleshchenkov, S.; Cheprakov, A. *New J. Phys.* **2008**, *10*, 013007.
(22) Kubatkin, S.; Danilov, A.; Hjort, M.; Cornil, J.; Bredas, J.-L.; Stuhr-Hansen, N.; Hedegard, P.; Bjornholm, T. *Nature* **2003**, *425*, 698–701.
(23) Kotov, N. A.; Stellacci, F. *Adv. Mater.* **2008**, *20*, 4221–4222.
(24) Sariciftci, N. S.; Smilowitz, L.; Heeger, A. J.; Wudl, F. *Science* **1992**, *258*, 1474–1476.
(25) Yu, G.; Gao, J.; Hummelen, J. C.; Wudl, F.; Heeger, A. J. *Science* **1995**, *270*, 1789–1791.
(26) Halls, J. J. M.; Walsh, C. A.; Greenham, N. C.; Marseglia, E. A.; Friend, R. H.; Moratti, S. C.; Holmes, A. B. *Nature* **1995**, *376*, 498–500.
(27) Snaith, H. J.; Whiting, G. L.; Sun, B. Q.; Greenham, N. C.; Huck, W. T. S.; Friend, R. H. *Nano Lett.* **2005**, *5*, 1653–1657.
(28) Crooker, S. A.; Hollingsworth, J. A.; Tretiak, S.; Klimov, V. I. *Phys. Rev. Lett.* **2002**, *89*, 186802.
(29) Nedelcu, M.; Lee, J.; Crossland, E. J. W.; Warren, S. C.; Orilall, M. C.; Guldin, S.; Huttner, S.; Ducati, C.; Eder, D.; Wiesner, U.; Steiner, U.; Snaith, H. J. *Soft Matter* **2009**, *5*, 134–139.
(30) Kersting, R.; Lemmer, U.; Deussen, M.; Bakker, H. J.; Mahrt, R. F.; Kurz, H.; Arkhipov, V. I.; Bassler, H.; Gobel, E. O. *Phys. Rev. Lett.* **1994**, *73*, 1440–1443.
(31) Westenhoff, S.; Daniel, C.; Friend, R. H.; Silva, C.; Sundström, V.; Yartsev, A. *J. Chem. Phys.* **2005**, *122*, 094903.
(32) Scholes, G. D.; Rumbles, G. *Nat. Mater.* **2006**, *5*, 683–796.
(33) Kersting, R.; Lemmer, U.; Mahrt, R. F.; Leo, K.; Kurz, H.; Bässler, H.; Gobel, E. O. *Phys. Rev. Lett.* **1993**, *70*, 3820–3823.
(34) Scholes, G. D. *Annu. Rev. Phys. Chem.* **2003**, *54*, 57–87.
(35) Meskers, S. C. J.; Hubner, J.; Oestreich, M.; Bässler, H. *Chem. Phys. Lett.* **2001**, *339*, 223–228.
(36) Devi, L. S.; Al-Suti, M. K.; Dosche, C.; Khan, M. S.; Friend, R. H.; Kohler, A. *Phys. Rev. B* **2008**, *78*, 045210.
(37) Ribierre, J. C.; Ruseckas, A.; Knights, K.; Staton, S. V.; Cumpstey, N.; Burn, P. L.; Samuel, I. D. W. *Phys. Rev. Lett.* **2008**, *100*, 017402.
(38) Nguyen, T. Q.; Martini, I. B.; Liu, J.; Schwartz, B. J. *J. Phys. Chem. B* **2000**, *104*, 237–255.
(39) Stevens, M. A.; Silva, C.; Russell, D. M.; Friend, R. H. *Phys. Rev. B* **2001**, *63*, 165213.
(40) Gesquiere, A. J.; Park, S. J.; Barbara, P. F. *J. Am. Chem. Soc.* **2005**, *127*, 9556–9560.
(41) Ferguson, A. J.; Kopidakis, N.; Shaheen, S. E.; Rumbles, G. *J. Phys. Chem. C* **2008**, *112*, 9865–9871.
(42) Zaushitsyn, Y.; Jespersen, K. G.; Valkunas, L.; Sundstrom, V.; Yartsev, A. *Phys. Rev. B* **2007**, *75*, 195201.
(43) Rothe, C.; King, S. M.; Monkman, A. P. *Phys. Rev. B* **2005**, *72*, 085220.
(44) Hertel, D.; Bassler, H.; Guentner, R.; Scherf, U. *J. Chem. Phys.* **2001**, *115*, 10007–10013.
(45) King, S. M.; Dai, D.; Rothe, C.; Monkman, A. P. *Phys. Rev. B* **2007**, *76*, 085204.
(46) Partee, J.; Frankevich, E. L.; Uhlhorn, B.; Shinar, J.; Ding, Y.; Barton, T. J. *Phys. Rev. Lett.* **1999**, *82*, 3673–3676.
(47) Gerhard, A.; Bassler, H. *J. Chem. Phys.* **2002**, *117*, 7350–7356.
(48) Giebink, N. C.; Sun, Y.; Forrest, S. R. *Org. Electron.* **2006**, *7*, 375–386.
(49) Gulbinas, V.; Mineviciute, I.; Hertel, D.; Wellander, R.; Yartsev, A.; Sundstrom, V. *J. Chem. Phys.* **2007**, *127*, 144907.
(50) Gadermaier, C.; Grasse, F.; Perissinotto, S.; Graf, M.; Galbrecht, F.; Scherf, U.; List, E. J. W.; Lanzani, G. *Phys. Rev. B* **2008**, *78*, 045207.
(51) Dhoot, A. S.; Greenham, N. C. *Phys. Rev. Lett.* **2003**, *91*, 219702.
(52) Lin, L. C.; Meng, H. F.; Shy, J. T.; Horng, S. F.; Yu, L. S.; Chen, C. H.; Liaw, H. H.; Huang, C. C.; Peng, K. Y.; Chen, S. A. *Phys. Rev. Lett.* **2003**, *90*, 036601.
(53) Schweitzer, B.; Arkhipov, V. I.; Scherf, U.; Bassler, H. *Chem. Phys. Lett.* **1999**, *313*, 57–62.
(54) Arias, A. C.; MacKenzie, J. D.; Stevenson, R.; Halls, J. J. M.; Inbasekaran, M.; Woo, E. P.; Richards, D.; Friend, R. H. *Macromolecules* **2001**, *34*, 6005–6013.

(type II heterojunction).[55] The samples are a well-studied model system for organic solar cells made of blended conjugated polymers.[12,14,54–58] Absorption of light creates singlet excitons, which may undergo a charge-transfer reaction at the interface between the two polymers. The charges may be further separated and transported to the electrodes by diffusion and by weak electric fields, they may recombine, or they may intersystem-cross into triplet excitons. The characteristic domain radius of the blend as prepared using chloroform as a solvent is 4.8 nm (ref 57) and is thus expected to strongly confine excitation migration and bimolecular interactions. We report the fluence dependence of time-resolved optical absorption and photoluminescence, and we demonstrate that nongeminate charge recombination is not important in this photovoltaic blend, but that bimolecular annihilations of singlet and triplet excitons by long-lived charge pairs are significant bimolecular decay channels. Surprisingly, we find that triplet−triplet annihilation, which we observed in a single-component film, is completely suppressed in the blend. We conclude that the efficiency of all bimolecular interactions is determined by the nanoscale morphology.

2. Photocycle in the Polyfluorene Blend

In this study, we investigate a 1:1 (by weight) blend of polyfluorene polymers poly(9,9-dioctylfluorene-*alt*-benzothiadiazole) (F8BT) and poly(9,9-dioctylfluorene-*co*-bis-*N*,*N*′-(4-butylphenyl)-bis-*N*,*N*′-phenyl-1,4-phenylene-diamine) (PFB) with molecular weights $M_w = 135$ kg/mol and $M_w = 150$ kg/mol, respectively (see Figure 1a for chemical structures). The films are spin-cast from chloroform. Our previous investigations of the same blend system have clarified the photocycle of the blend in the absence of bimolecular reactions (see Figure 1b).[18,55,57] The primary photoexcitations, singlet excitons, are efficiently split at the heterojunction into interfacial charge pairs within 20 ps.[57] The charge pairs (also termed "geminate charge pairs" or "polaron pairs" in the literature)[18,59] are immobile, and a subpopulation of them are emissive, with the photoluminescence maximum red-shifted from the exciton emission.[55] They may recombine geminately into neutral triplet excitons on F8BT (75%) or directly to the ground state (15%). A minority of charges (10%) becomes spatially separated (SSC) and is longer lived.[18] The yield of spatially separated charge pairs correlates well with the internal quantum efficiency measured at short-circuit conditions.[14,60] We note, however, that the internal quantum efficiency can be considerably increased by applying a reverse bias voltage.[60]

The various second-order interactions that could possibly occur in PFB:F8BT blends during and after excitation are now considered. To clarify this discussion, Figure 1b presents a graphical representation of the population evolution at low

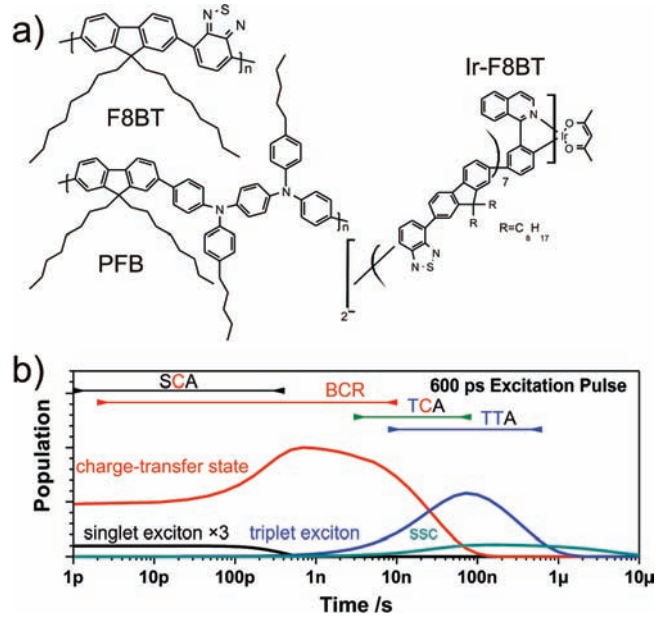

Figure 1. Panel (a) shows the chemical structures of F8BT, PFB, and [iridium(III) bis(1-(3′-(ω-(4‴,4‴,5‴,5‴-tetramethyl-1″,3″,2″-dioxaborolan-2″-yl)-oligo[9″,9″-dioctylfluorene-*alt*-benzothiadiazole)phenyl)isoquinolinato-*N*,*C*′)(acetyl acetonate)] (F8BT-Ir). Panel (b) indicates how the excited-state population evolves considering only monomolecular decay channels and following a laser pulse of 600 ps duration; see methods for rate equations. The time-scales for all bimolecular interactions that could occur at high excitation density are sketched. Abbreviations are SCA for singlet exciton-charge annihilation, BCR for nongeminate bimolecular charge recombination, TCA for triplet exciton−charge annihilation, and TTA for triplet exciton−triplet exciton annihilation.

intensity. In our experiments, the pulse length of the excitation laser was 600 ps and had an instantaneous intensity of 2.5×10^5 W/cm^2 at the highest energy used. This is 3 orders of magnitude lower than the threshold for singlet−singlet annihilation in F8BT films, which was determined to be 1×10^8 W/cm^2.[39] Therefore, an exciton will likely create a charge-transfer state before another photon is absorbed in its vicinity, and singlet−singlet annihilation will not occur. A high density of charge-transfer states is created during the excitation pulse, which means that singlet−charge annihilation (SCA) and bimolecular recombination of two interfacial charge pairs (BCR) could occur during the excitation pulse. At intermediate time-scales, from 1 to 100 ns, the gradual formation of triplet excitons from interfacial charge pairs leads to an overlap of the charge pair and triplet exciton populations. During this time, triplet excitons may be annihilated by charges (TCA), and bimolecular charge recombination could occur. These bimolecular interactions can be distinguished experimentally, because only the latter would shorten the photoluminescence decay at high excitation densities, which monitors the population of interfacial charge pairs. The former, TCA, could only be observed in the fluence dependence of the transient absorption, because the charge population is not changed. At long time-scales, after 100 ns, the excited-state population is dominated by triplet excitons, with a minor contribution from charges that have become spatially separated. Fluence-dependent transient absorption dynamics would indicate triplet−triplet annihilation (TTA). As illustrated, the fluence dependence of the photoluminescence and induced absorption on the various time ranges (<1 ns, 1−100 ns, and >100 ns) will allow individual determination of the various second-order interactions.

(55) Morteani, A. C.; Dhoot, A. S.; Kim, J. S.; Silva, C.; Greenham, N. C.; Murphy, C.; Moons, E.; Cina, S.; Burroughes, J. H.; Friend, R. H. *Adv. Mater.* **2003**, *15*, 1708–1712.
(56) Morteani, A. C.; Sreearunothai, P.; Herz, L. M.; Friend, R. H.; Silva, C. *Phys. Rev. Lett.* **2004**, *92*, 247402.
(57) Westenhoff, S.; Howard, I. A.; Friend, R. H. *Phys. Rev. Lett.* **2008**, *101*, 016102.
(58) Campbell, A. R.; Hodgkiss, J. M.; Westenhoff, S.; Howard, I. A.; Marsh, R. A.; McNeill, C. R.; Friend, R. H.; Greenham, N. C. *Nano Lett.* **2008**, *8*, 3942–3947.
(59) Huang, Y.-S.; Westenhoff, S.; Avilov, I.; Sreearunothai, P.; Hodgkiss, J. M.; Deleener, C.; Friend, R. H.; Beljonne, D. *Nat. Mater.* **2008**, *7*, 483–489.
(60) Gonzales-Rabbade, A.; Morteani, A.; Friend, R. H. *Adv. Mater.* **2009**, *21*, 3924–3927.

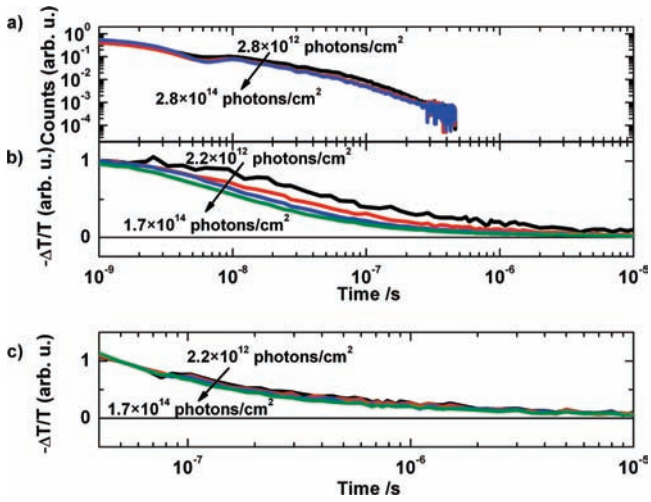

Figure 2. Panel (a) shows the normalized time-resolved photoluminescence at 650 nm for the fluences 2.8×10^{12} (black), 2.8×10^{13} (red), and 2.8×10^{14} photons/cm^2 (blue). Panel (b) shows the normalized transient absorption at 650 nm probe wavelength for the fluences 2.2×10^{12} (black), 4.7×10^{13} (red), 1.2×10^{14} (blue), and 1.7×10^{14} photons/cm^2 (green). Panel (c) shows the transient absorption data for all fluences normalized to their value at 40 ns.

3. Triplet−Charge Annihilation, Absence of Bimolecular Charge Recombination, and Triplet−Triplet Annihilation

We present the fluence dependence of the time-resolved photoluminescence and the transient induced absorption in Figure 2a and b, respectively. We highlight that we use the same excitation laser (AOT-YVO-25QSPX, Advanced Optical Technologies Ltd.: pulse length 600 ps, $\lambda_{exc} = 355$ nm) for both measurements, to ensure identical excitation conditions and enable direct comparison of the fluence dependencies. At the detection wavelength of 650 nm, the photoluminescence is a selective probe of the charge-transfer state population, and its decay rate is independent of excitation density. This implies that bimolecular charge recombination, which would reduce the lifetime of the interfacial charge pairs at high excitation density, does not take place. Figure 2b shows that the decay of the transient absorption signal at 650 nm, which probes a combination of the interfacial charge pair and triplet exciton populations,[18] is strongly fluence dependent at the same time-scale. Given we have just observed that the charge-transfer state decay is independent of fluence, this implies that the triplet decay must depend on fluence. In general, triplet−triplet annihilation results in a singlet exciton that should ionize efficiently at the heterojunction and reform a charge-transfer state. Triplet−charge annihilation simply quenches the triplet exciton, and the charge is retained. Thus, the independence of the photoluminescence decay rate on excitation density also implies that interfacial charge pairs are not being reformed as the eventual product of any bimolecular interaction. This suggests that triplet−triplet annihilation is not occurring on this time-scale, because this process would yield a singlet exciton, which would subsequently reform a charge-transfer state. Therefore, we conclude that the second-order kinetics in the 1−100 ns time window are due to triplet−charge annihilation and that triplet−triplet annihilation is negligible. This conclusion is further confirmed by the observation that the transient absorption decay becomes fluence independent after 100 ns (see Figure 2c) when the excited-state population is predominantly triplet excitons.

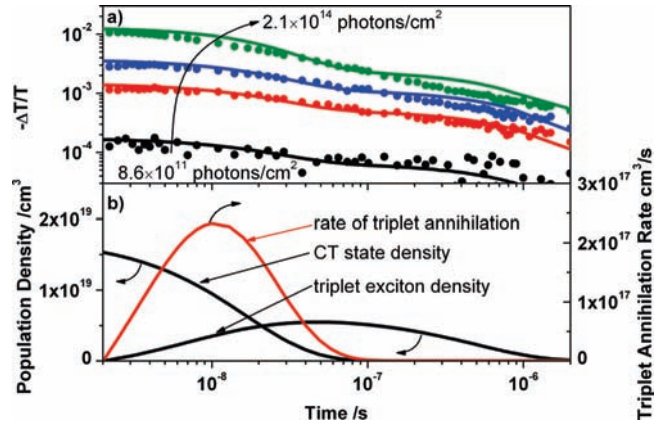

Figure 3. Panel (a) shows the transient absorption of the PFB:F8BT blend at excitation fluences of 8.6×10^{11}, 6.9×10^{12}, 1.7×10^{13}, and 2.1×10^{14} photons/cm^2 (black, red, blue, and green symbols, respectively). The global fit described in the text is shown as the lines with the same color code. Panel (b) presents the density of triplets and charges for the highest excitation fluence as extracted from the global fit. On the right axis, the rate of triplet annihilation (triplet−charge annihilation+triplet−triplet annihilation) is shown (red line) for the same fluence.

To extract quantitative information regarding the annihilation processes, we fit the transient absorption signal to a kinetic model. The transient absorption at a given time is:

$$\Delta T/T = (\sigma_{CT} \cdot ([CT] + [SSC]) + \sigma_T \cdot [T]) l_{film} \qquad (1)$$

where $\sigma_{CT} = 4.3 \times 10^{-16}$ cm^2 and $\sigma_T = 1.1 \times 10^{-16}$ cm^2 are the absorption cross sections of interfacial charge pairs and triplet excitons at 650 nm, respectively,[18] [CT] is the charge-transfer state population, [SSC] is the population of spatially separated charge pairs, [T] is the triplet state population, and l_{film} is the film thickness (140 nm as measured by profilometry). The decay of the SSC population occurs on a time-scale greater than 1 μs (see long tail in Figure 2c), so it is neglected in this analysis. The population decay of interfacial charge pairs does not depend on fluence, and we therefore model its time dependence as previously described (eqs 1 and 3 in ref 18). The evolution of the triplet population, on the other hand, does depend on fluence and is expressed as

$$d[T]/dt = k_{CT\rightarrow T}[CT] - k_{T\rightarrow GS}[T] - \gamma_{TTA}[T]^2 - \gamma_{TCA}[T][CT] \qquad (2)$$

where $k_{CT\rightarrow T} = 2.6 \times 10^7$ s^{-1} is the rate of transfer from the charge pairs to the triplet state,[18] $k_{T\rightarrow GS}$ is the monomolecular triplet relaxation rate, γ_{TTA} is the bimolecular triplet−triplet annihilation constant, and γ_{TCA} is the bimolecular triplet−charge annihilation constant. We note that the direct generation of triplet excitons from singlet excitons is inefficient in this polymer blend and was therefore omitted in eq 2.[61]

The transient absorption data are globally fit at all fluences (using minimization of least-squares in MATLAB, Mathworks Inc.) by varying the parameters γ_{TTA}, γ_{TCA}, and k_{TR} to minimize the residual between the observed data and eq 1, which is solved by numerically integrating the population equations. The fit is in good agreement with the data over an order of magnitude in fluence and 3 orders of magnitude in time (see Figure 3a). The extracted parameters (with 90% confidence bounds shown in brackets) are: $k_{T\rightarrow GS} = 9.8 \times 10^5$ s^{-1} ($(9.7-10) \times 10^5$ s^{-1}), $\gamma_{TTA} = 1 \times 10^{-15}$ cm^3/s ($(0-2) \times 10^{-15}$ cm^3/s), and $\gamma_{TCA} =$

(61) Ford, T. A.; Avilov, I.; Beljonne, D.; Greenham, N. C. *Phys. Rev. B* **2005**, *71*, 125212.

5.6×10^{-12} cm^3/s ($(5.3-5.8) \times 10^{-12}$ cm^3/s). The monomolecular triplet decay rate ($k_{T\rightarrow GS}$) agrees well with previous measurements.[62] To visualize these results, Figure 3b presents the charge and triplet populations together with the total rate of triplet annihilation, which is the sum of charge−triplet and triplet−triplet annihilations. This analysis confirms our qualitative analysis, in that triplet−charge annihilation is much more significant than triplet−triplet annihilation.

4. Triplet−Triplet Annihilation in Pristine Films of F8BT-Ir

The lack of triplet−triplet annihilation is surprising given that it can be so significant in single-component films of pristine conjugated polymers.[44,48] Indeed, triplet−triplet annihilation has been studied on millisecond time-scales over a range of temperatures <170 K in pristine films of poly(9,9-dihexylfluorene-*co*-benzothiadiazole) (F6BT), which differs from F8BT only in the length of the side chains.[63] Using this reported bimolecular recombination rate along with its temperature dependence, we should expect triplet−triplet annihilation with a bimolecular recombination coefficient of approximately $\gamma_{TTA} = 5 \times 10^{-12}$ cm^3/s at ambient temperature. To independently ascertain why triplet−triplet annihilation is absent in the blend, we studied this process in a pristine F8BT film. However, very few triplets are formed in pure F8BT, because the decay rate of singlet excitons is much greater than the intersystem crossing rate.[61] We overcome this obstacle by utilizing a single-component film of F8BT-Ir, in which F8BT oligomers are covalently attached to a cyclometalated iridium complex (see Figure 1 for chemical structure). The synthesis has previously been reported, along with a demonstration that singlet excitons, which are generated by optical excitation of the F8BT sites, intersystem cross at the iridium sites into the triplet manifold, and transfer back to the F8BT sites.[18] The generation of F8BT−triplet excitons occurs on time-scales <1 ns and with unity yield, which implies that charges and singlet excitons are absent on the time-scales that are investigated in this study.

To study the dynamics of the triplet excitons in this thin sensitized oligomer film, we excite the F8BT-Ir at 400 nm with a 100 fs laser pulse and then monitor the ground-state bleach of the F8BT-Ir absorption at 355 nm using the 600 ps laser pulses as a probe. Under these excitation conditions, high singlet exciton densities could be created, and singlet−singlet annihilation, which produces undesired charge species,[39] might occur before the triplets are generated. We ascertain that this is not the case by plotting the initially measured transient absorption as a function of fluence in Figure 4a. We find that the initial signal scales linearly with fluence for $<2.5 \times 10^{13}$ photon/cm^2, indicating that triplets are formed faster than bimolecular singlet−singlet annihilation in this regime. At higher fluences, the dependence becomes sublinear, which is the signature of singlet−singlet annihilation. We restrict the subsequent analysis to fluences that fall into the linear regime.

Figure 4b shows normalized decays of the F8BT absorption bleach taken at high and low fluence within the linear regime for times >1 ns. The signal is exclusively caused by the triplet population. The data show that, in contrast with our observations in the blend, the triplet population decay is fluence dependent

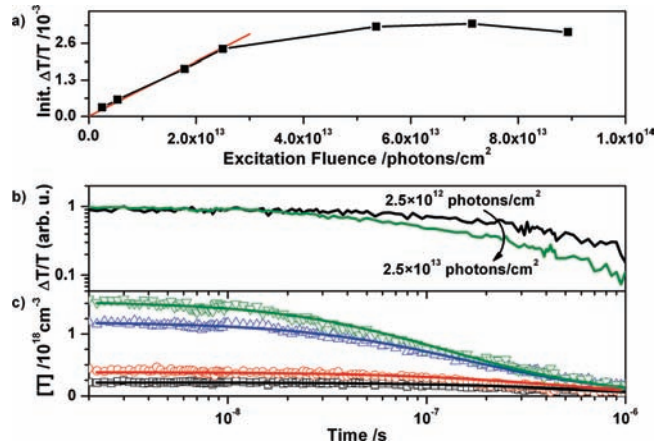

Figure 4. Panel (a) presents the absorption bleach 1 ns after photoexcitation at 355 nm probe wavelength of an F8BT-Ir film as a function of excitation pulse fluence. Panel (b) shows the normalized decay of the absorption bleach for the highest and lowest fluence in the linear regime (0.25×10^{13} and 2.5 photons/cm^2) as the black and green lines, respectively. Panel (c) shows the decay of the absorption bleach (translated into triplet density) for all four excitation fluences in the linear regime (0.25×10^{13}, 0.5×10^{13}, 1.2×10^{13}, and 2.5×10^{13} photons/cm^2 as black □, red ○, blue △, and green ▽, respectively). The solid lines show the global fit discussed in the text.

in this single-component film, indicating that in this case triplet−triplet annihilation does occur. Using the known excitation fluence, extinction coefficient, and film thickness, we translate the induced absorption into triplet densities (Figure 4c).

To quantitatively examine triplet−triplet annihilation in the F8BT-Ir, we use the rate equation for the triplet density as

$$d[T]/dt = -k_{T\rightarrow GS}[T] - \gamma_{TTA}[T]^2 \quad (3)$$

The nomenclature remains as previously introduced. This rate equation can be integrated, and the analytic expression for the triplet density as a function of time is

$$[T](t) = T_0 \exp(-k_{T\rightarrow GS}t)/(1 + (T_0\gamma_{TTA}/k_{T\rightarrow GS}) \times (1 - \exp(-k_{T\rightarrow GS}t)) \quad (4)$$

where T_0 is the initial triplet density. We globally fit the data (symbols in Figure 4c) to this expression (lines in Figure 4c), and the extracted parameters are: $\gamma_{TTA} = 5 \times 10^{12}$ cm^3/s and $k_{T\rightarrow GS} = 5 \times 10^5$ s^{-1}. The value for γ_{TTA} is consistent with the previous report on F6BT,[63] and the value of $k_{T\rightarrow GS}$ is similar to that previously reported for a single component F8BT film.[62]

As an additional consideration, we examine what the extracted bimolecular coefficients imply about the triplet exciton diffusion coefficient and diffusion lengths. Assuming that annihilation is controlled by three-dimensional diffusion, the triplet diffusion coefficient can be calculated from the bimolecular annihilation constant as $D = \gamma_{TTA}/(8\pi \cdot r_{TTA}^{crit})$,[64] where D is the diffusion constant and r^{crit} is the critical radius for the interaction. Assuming that r^{crit} is 1 nm, the triplet diffusion coefficient in the pristine F8BT-Ir is 1.6×10^{-6} cm^2/s. From the diffusion coefficient, the diffusion length can be estimated as $d = 2\sqrt{(Dt)}$. Given the monomolecular lifetime of the triplet is approximately 2 μs, the triplet diffusion length is approximately 15 nm. This is comparable to a typical singlet exciton diffusion length,[57] which is rationalized by considering that while triplet excitons have lifetimes that are 3 orders of magnitude longer than singlet excitons, they also have diffusion rates that are 3 orders of

(62) Ohkita, H.; Cook, S.; Ford, T. A.; Greenham, N. C.; Durrant, J. R. *J. Photochem. Photobiol., A* **2006**, *182*, 225–230.
(63) Westerling, M.; Vijila, C.; Österbacka, R.; Stubb, H. *Synth. Met.* **2003**, *139*, 843–845.
(64) Powell, R. C.; Soos, Z. G. *J. Lumin.* **1975**, *11*, 1–45.

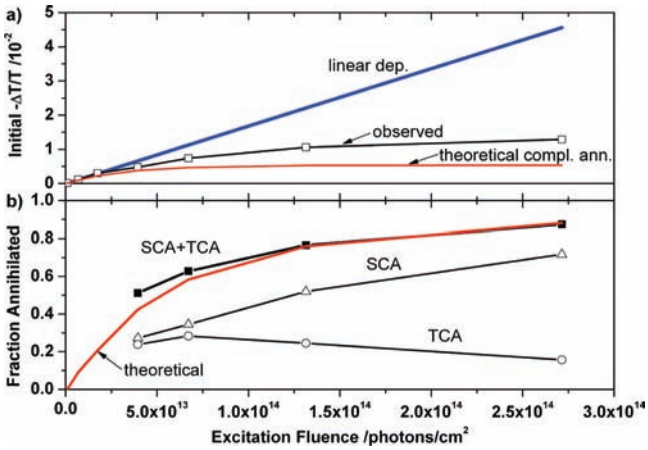

Figure 5. Panel (a) shows the measured transient absorption of the PFB:F8BT blend at 1 ns (black line with □), the expected absorption based on a linear fit of the first three data points ("case 1", blue line), and the initial transient absorption expected if complete annihilation occurred ("case 2", red line). See text (section 6) for further details. Panel (b) shows the measured fraction of total absorbed photons that annihilate due to singlet−charge annihilation (black line with △), triplet−charge annihilation (black line with ○), and the combination of singlet−charge annihilation and triplet−charge annihilation (black line with ■). The theoretical fraction of annihilation assuming all excitations in a domain after the first are annihilated is shown as the red line ("case 2").

magnitudes slower. This is consistent with recent results showing that in thin films of small organic molecules, singlet and triplet exciton diffusion lengths are similar.[65]

With regard to the initial question of triplet−triplet annihilation in nanostructured blends, these measurements clearly show that triplet−triplet annihilation is active in pristine F8BT films and that the triplet diffusion length is larger than the average domain size in the blends. Because we found triplet−triplet annihilation to be absent in the blends, we conclude that the nanoscale blend morphology must severely restrict the triplet diffusivity and therefore also limits the probability of triplet−triplet annihilation. This conclusion will be the basis for the model that we describe in section 6.

5. Picosecond Time-Scales: Singlet−Charge Annihilation

We now return to analyze in detail the second-order kinetics of the blend during the excitation pulse. To investigate singlet−charge annihilation, we present the magnitude of the transient absorption signal at $t = 1$ ns as a function of fluence in Figure 5a (open symbols). The data scale sublinearly with fluence. At this time delay, the induced absorption is due only to charges (see Figure 1b), and the data reflect the outcome of any bimolecular interaction that may occur for times $t < 1$ ns, that is, during the excitation pulse (600 ps). Singlet−singlet annihilation, singlet−charge annihilation, and bimolecular charge recombination could occur in this time regime. As explained previously, singlet−singlet annihilation is precluded due to low instantaneous intensity of the excitation pulse. From our observation of the fluence independence of the photoluminescence decay rate (Figure 2a), it is clear that bimolecular charge recombination is not occurring. This leaves only singlet−charge annihilation to explain the observed second-order effect.

The straight line in Figure 5a shows the expected induced absorption based on a linear fit of the transient absorption of the three lowest excitation fluences. The fraction of excitons that undergo singlet−charge annihilation at a given fluence, calculated by comparing the observed and expected induced absorption, is plotted in Figure 5b as "△". It is clear that singlet−charge annihilation significantly reduces the fraction of excitons that create interfacial charge pairs at high fluence, with approximately 60% of excitons annihilating at the highest fluences. Knowing the fraction of excitons that are quenched by singlet−charge annihilation, and also knowing the competitive rate of charge transfer,[57] we can estimate the rate constant for bimolecular singlet−charge annihilation to be on the order of 10^{-9} cm^3/s (see Methods for details). We suggest that this process may be so efficient not only because excitons are highly mobile, but also because the spectral overlap between the exciton emission and the charge-induced absorption may facilitate longer range Förster transfer of the exciton to the annihilating charge.[66]

6. Bimolecular Interactions in Confined Geometries

We now consider how morphology limits the bimolecular interactions that we observe in the polyfluorene blend. The binary blend is divided into F8BT and PFB polymer domains, and we propose that excitation transfer is inhibited between F8BT domains. Singlet excitons ionize at the domain boundaries to form charge pairs within ∼20 ps, which in turn generate triplet excitons within ∼40 ns.[18] If a singlet exciton is generated in a polymer domain that already contains a charge pair, singlet−charge annihilation may occur. However, this process directly competes with exciton ionization, and thus some domains may contain multiple charge pairs after the excitation pulse. In this case, triplet−charge annihilation may occur, after one of the charge pairs has converted into a triplet exciton. This process is expected to be active until a single charge pair remains in each domain. This ultimate charge pair will eventually create a triplet exciton that singly occupies the F8BT domain, and, if its diffusion is strongly restricted by the morphology, is constrained to decay monomolecularly. Therefore, all save one excitation in a multiply excited domain can decay through a bimolecular process. The probability of multiple excitations being created in a given domain can be found by using Poisson statistics:

$$P[N = k] = \alpha^k \exp(-\alpha)/k! \tag{5}$$

$P[N = k]$ is the probability that exactly k excitations reside in a domain, and α is the average number of excitations per domain, which we calculate on the basis of the pump fluence and the known average domain radius of 4.8 nm.[57] Poisson statistics is the appropriate method to calculate the domain occupancies, because the number of photons absorbed in a given domain is discrete, photon absorption is independent of the number photons already absorbed in that domain, and the average excitation density is known. The maximum fraction of the excited-state population that could annihilate is then given by

$$\langle \mathrm{BA} \rangle = \frac{\sum_{i=1}^{\infty} i \times P[N = (i+1)]}{\sum_{i=1}^{\infty} i \times P[N = i]} \tag{6}$$

(65) Lunt, R. R.; Giebink, N. C.; Belak, A. A.; Benziger, J. B.; Forrest, S. R. *J. Appl. Phys.* **2009**, *105*, 053711.

(66) Hodgkiss, J. M.; Tu, G. L.; Albert-Seifried, S.; Huck, W. T. S.; Friend, R. H. *J. Am. Chem. Soc.* **2009**, *131*, 8913–8921.

where the numerator gives the number of excitations that can annihilate, which is all but one in every multiply excited domain, and the denominator gives the total number of excitations. It is instructive to consider the extreme cases: (1) the case where annihilation is switched off and (2) the case where annihilation is complete within a domain, leaving it singly occupied. The theoretical initial transient absorption in case (1) is simply the linear extrapolation of the experimental data points that fall into the linear regime in Figure 5a, shown as a blue line. The transient absorption for case (2) is then calculated by multiplying the blue line found in case (1) by one minus the maximum fraction that can annihilate found by evaluating expression 5 (with N truncated at 100). The resulting predicted transient absorption for case (2) is shown as the red line in Figure 5a. The experimentally determined transient absorption at 1 ns delay time (black line and "□" in Figure 5a) falls between the two extreme cases. We recall that at this delay time, singlet−charge annihilation is completed, but that triplets have not yet formed. Thus, this shows that some domains are still multiply occupied by charge pairs after the 600 ps excitation pulse.

To quantitatively assess the efficiency of triplet−charge annihilation, we illustrate the model in a different representation in Figure 5b, where the fraction of all excitations that are deactivated by an annihilation reaction is plotted. For case (1), where annihilation is switched off, this fraction is 0 (not shown), and for case (2), where all but one excitation are assumed to be annihilated within a single polymer domains, the result is shown as the red curve. The experimental data are presented as "△" and "○" for the fraction of photoexcitations that decays by singlet−charge annihilation (see section 5) and by triplet−charge annihilation, respectively. The latter data are calculated from our fits of the experimental transient absorption data (see eq 11 in Methods). The sum of these two fractions then gives the total fraction of initial excited-state population that is observed to decay bimolecularly. We see that the measured total fraction is accurately described by the model, clearly suggesting that bimolecular interactions are efficient, but confined to individual polymer domains. Within the polymer domains, singlet−charge annihilation and triplet−charge annihilation efficiently reduce all multiple excitations to single excitations.

7. Discussion and Implications for Device Physics

In section 3, we demonstrated that bimolecular charge recombination does not occur in F8BT:PFB blends. This is a striking result considering that the average distance between charge pairs is only approximately 4.5 nm at the highest density in our measurements. The finding is in contrast to polymer:PCBM blends, where substantial bimolecular charge recombination was found on comparable time-scales and similar excitations densities.[16] However, it is consistent with our previous reports[18,59,60] and is readily explained by that the charge pairs are immobile in PFB:F8BT blends.[18] Thus, the occurrence of bimolecular charge recombination depends on the choice of materials. We note that the exact mechanism of bimolecular charge recombination still remains unclear. In such an event, the electron and holes would reside on different polymer domains and must re-form a charge pair prior to recombination. The observation of an increased charge recombination rate at high excitation densities, as reported in ref 16, implies that the sites at the heterojunction that are initially populated stabilize the interfacial charge pair, whereas at others sites, where bimolecular charge recombination could take place, the interfacial charge pair is destabilized, and faster charge recombination may occur. Such local differences are in line with recent predictions, in which it was found that the stability of the exciton versus charge-transfer state depends on the local arrangement of polymer chains across the heterojunction,[59] but further research is needed to clarify this mechanism.

An unexpected implication of the absence of bimolecular charge pair recombination is that the F8BT:PFB blend can support an extremely high charge-transfer state density. In our measurements, its density is over an order of magnitude greater than the singlet exciton population threshold for annihilation, and it is limited only by the occurrence of singlet−charge annihilation prior to exciton ionization at the heterojunction.[39] This is due to the fact that singlet excitons are very mobile and annihilate, while most of the charge pairs are bound across the interface and immobile.[18] In organic lasers, high excitation densities are necessary, and singlet−singlet annihilation is an efficiency limiting process.[5] The utilization of high density long-lived interfacial charge pairs, either as an active population or as a storage pool, may prove useful to circumvent this problem.

Finally, we comment on our measurements of the triplet diffusion length in F8BT-Ir films. Some investigations have sought to relax the geometrical constraints on organic solar cell morphology by quickly converting singlet excitons to triplet excitons. The assumption was that triplet excitons could diffuse further than singlet excitons to an ionizing interface.[67] Our results suggest that the diffusion lengths of triplet and singlet excitons are similar, and thus using a triplet exciton as the ionizable species will not necessarily relax the morphological constraints.

8. Summary

Our findings demonstrate that in a conjugated polymer photovoltaic blend bimolecular recombination between charges is not a significant decay mechanism, which is reasonable considering that the majority of charge pairs are immobile. We have demonstrated that unusually high charge-transfer state densities can be sustained. Triplet excitons are mobile, but their diffusion is strongly constrained by the blend morphology. This strong restriction of triplet motion effectively turns off triplet−triplet annihilation in a nanostructured blend. The dominant second-order loss mechanisms are singlet−charge annihilation on picosecond time-scales, followed by triplet−charge annihilation on nanosecond time-scales. Both of these mechanisms occur predominantly in domains of the blend that become multiply occupied during the excitation pulse, and therefore the morphology also plays a key role in determining their efficiency. Consideration of these bimolecular interaction mechanisms is important for understanding and engineering the function of organic solar cells and organic optoelectronic devices that require high excited-state densities, such as light-emitting diodes, light-emitting transistors, and organic lasers.

9. Methods

Films were spin-cast at 3000 rpm from 10 mg/mL (total weight) chloroform solutions resulting in thicknesses on the order of 140 nm as measured by profilometry. F8BT-Ir was prepared according to the previously published procedure.[18] Transient absorption measurements were performed using the third harmonic output (355 nm) of a Q-switched Nd:YVO_4 laser (ACE; Advanced Optical Technologies Ltd.) as the excitation source. The 650 nm probe was generated by a home-built NOPA pumped by the 1 kHz, 800 nm output of a sub 100 fs regenerative amplifier (Spitfire; Spectra-

(67) Shao, Y.; Yang, Y. *Adv. Mater.* **2005**, *17*, 2841–2844.

Physics). Details of the detection system are described elsewhere.[18] The time delay between the pump and probe was controlled by an electronic delay generator (DG-565, Standford Research Systems) triggered by every second synchronization pulse from the amplifier. Time correlated single photon counting (TCSPC) was performed using the same Nd:YVO_4 laser as an excitation source and with a setup described previously.[68,69]

The time-dependencies of the population of the singlet excitons (E), the interfacial charge pairs (CT), the triplet excitons (T), and the spatially separated charge pairs (SSC) are described as

$$\frac{dE}{dt} = g(t) - k_{S\to CT}E - \gamma_{SSA}E^2 - \underbrace{\gamma_{SCA}E\times CT}_{bimolecular} \tag{7}$$

$$\frac{dCT}{dt} = k_{S\to CT}E - k_{CT\to T}CT - k_{CT\to SSC}CT - k_{CT\to GS}CT - \underbrace{\gamma_{BCR}CT^2}_{bimolecular} \tag{8}$$

$$\frac{dT}{dt} = k_{CT\to T}CT - k_{T\to GS}T - \underbrace{\gamma_{TTA}T^2 - \gamma_{TCA}T\times CT}_{bimolecular} \tag{9}$$

$$\frac{dSSC}{dt} = k_{CT\to SSC}CT - \underbrace{\gamma_{BSSC}SSC^2}_{bimolecular} \tag{10}$$

$k_{A\to B}$ representing the monomolecular rate constant for population change from state A to B; γ_{SSA} is the previously determined singlet−singlet annihilation rate constant;[39] and γ_{SCA}, γ_{BCR}, γ_{TTA}, γ_{TCA}, and γ_{BSSC} represent the bimolecular rate constant for singlet-charge annihilation, bimolecular interfacial charge pair annihilation, triplet−triplet annihilation, triplet charge annihilation, and bimolecular recombination of spatially separated charge pairs. Figure 1b shows the numerically determined solutions to eqs 7−10, with only the monomolecular terms considered. $g(t)$ is a 600 ps fwhm Gaussian pulse centered at $t = 0$. Once the evolutions of the triplet and charge pair populations are known at each fluence from globally fitting the model based on eqs 7−10 to the transient absorption data, the fraction of triplets that decay due to triplet−charge annihilation is determined at each fluence as

$$\frac{\int_0^\infty \gamma_{TCA}T\times CT\,dt}{\int_0^\infty k_{T\to GS}T + \gamma_{TCA}T\times CT\,dt} \tag{11}$$

The singlet exciton−charge bimolecular coefficient (γ_{sca}) (section 5) can be estimated using the known fraction of excitations that undergo singlet exciton−charge annihilation (F_{sca}) (see Figure 5b), the competitive rate of charge-transfer ($k_{CT} = 1\times10^{11}$ s^{-1}),[57] and the approximate charge density during the pulse (C; we use the initial value for the charge density extracted from the modeling shown in Figure 3). We then solve

$$F_{sca} = \frac{\gamma_{sca}C}{\gamma_{sca}C + k_{ct}} \tag{12}$$

for γ_{sca} at each of the measured intensities. All values fall into the range between $\gamma_{sca} = 1\times10^{-9}$ cm^3/s and $\gamma_{sca} = 10\times10^{-9}$ cm^3/s.

The 90% confidence intervals given on fitting parameters in section 3 correspond to the minimum and maximum values of the parameter p for which $SSR(p) < SSR\cdot(1 + F/(N - P))$ holds. SSR stands for the sum of squares of differences between the data and the fit. SSR and SSR(p) are minimized for all parameters and for all parameters except p, respectively. N denotes the number of data points, and P is the number of parameters. F is the F-distribution value, calculated for the confidence interval (90%) and the degrees of freedom 1 and $N - P$.

Acknowledgment. We acknowledge financial support from EPSRC. H.A.B. and C.K.W. acknowledge EPSRC grant EP/C548132/1. S.W. thanks Fitzwilliam College Cambridge for a Junior Research Fellowship and the EU commission for an Intra European Fellowship, and I.A.H. thanks the Cambridge Commonwealth Trust for financial support.

JA908046H

(68) Schmidtke, J. P.; Kim, J.-S.; Gierschner, J.; Silva, C.; Friend, R. H. *Phys. Rev. Lett.* **2007**, *99*, 167401.

(69) Silva, C.; Russell, D. M.; Dhoot, A. S.; Herz, L. M.; Daniel, C.; Greenham, N. C.; Arias, A. C.; Setayesh, S.; Mullen, K.; Friend, R. H. *J. Phys.: Condens. Matter* **2002**, *14*, 9803–9824.